phys. stat. sol. (a) **40**, 447 (1977)

Subject classification: 1.2 and 18.4; 22.8.1

Mineralogisches Institut der Universität Bonn,
Lehrstuhl für Mineralogie und Kristallographie[1]) *(a) and*
Philips Research Laboratories, Eindhoven (b)

The High-Temperature Polymorph β-$FeSO_4$

Stability, Magnetic Structure, and Magnetic Properties

By

A. KIRFEL (a), W. SCHÄFER (a), G. WILL (a), and K. H. J. BUSCHOW (b)

The p–T-phase diagram of anhydrous iron sulfate $FeSO_4$ is investigated by high pressure–high temperature experiments up to 15 kbar and 800 °C. The experiments yield a high-temperature polymorph β-$FeSO_4$ (space group Pbnm). The magnetic properties are studied by susceptibility measurements, which indicate an antiferromagnetic transition temperature of $T_N = 14$ K. The antiferromagnetic structure is determined from neutron diffraction powder data. The magnetic moments are perpendicular to the c-axis, and within (001) planes they are inclined by $(41 \pm 4)°$ towards a_0. There are ferromagnetic (110) planes with an antiferromagnetic propagation vector [110]. The Fe^{2+} moments are $\mu = 5.44\mu_B$ from neutron diffraction data at 4.2 K and $\mu_{eff} = 5.32\mu_B$ from magnetization measurements.

Das p–T-Phasendiagramm von wasserfreiem Eisensulfat $FeSO_4$ wird bei Hochdruck–Hochtemperaturexperimenten bis zu 15 kbar und 800 °C untersucht. Die Experimente ergeben ein Hochtemperatur-Polymorph β-$FeSO_4$ (Raumgruppe Pbnm). Die magnetischen Eigenschaften werden mit Suszeptibilitätsmessungen untersucht, die eine antiferromagnetische Übergangstemperatur von $T_N = 14$ K ergeben. Die antiferromagnetische Struktur wird aus Daten von Neutronenbeugung an Pulverproben bestimmt. Die magnetischen Momente sind senkrecht zur c-Achse; innerhalb der (001)-Ebenen sind sie mit $(41 \pm 4)°$ gegen a_0 gekippt. Es existieren ferromagnetische (110)-Ebenen mit einem antiferromagnetischen Ausbreitungsvektor [110]. Die Fe^{2+}-Momente betragen $\mu = 5{,}44\mu_B$ aus Neutronenbeugungswerten bei 4,2 K und $\mu_{eff} = 5{,}32\mu_B$ aus Magnetisierungsmessungen.

1. Introduction

The magnetic properties of sulfates MSO_4 containing 3d-transition elements were studied as early as 1911 by Kamerlingh Onnes and his coworkers [1]. Susceptibility measurements and especially neutron diffraction experiments in the sixties revealed their antiferromagnetic spin configurations [2]. In the course of these and later studies it was realized that all sulfates MSO_4, and also the corresponding selenates $MSeO_4$ crystallize in two polymorphic forms, a low-pressure, high-temperature modification (β-MSO_4) of symmetry Pbnm-D_{2h}^{16}, and a more dense high-pressure, low-temperature polymorph (α-MSO_4) of the higher symmetry Cmcm-D_{2h}^{17}. In the systematic study of the polymorphism of these compounds we have reported previously the p–T phase diagram of $MnSeO_4$ [3] and a phase study of $MnSO_4$ [4]. The antiferromagnetic structures for α-$MnSeO_4$ [3], β-$MnSeO_4$ [5], α-$MnSO_4$ [6], and for α-$FeSO_4$ [7] were determined by neutron diffraction. The β-phase of $MnSO_4$ could not be quenched [4].

In this paper we wish to report the phase diagram of $FeSO_4$ and the magnetic properties including the magnetic structure of the low-pressure β-$FeSO_4$ polymorph.

---

[1]) 5300 Bonn, BRD.

2. Preparation

α-$FeSO_4$ was synthesized by dehydration of $FeSO_4 \cdot 7\,H_2O$ at 300 °C. Under these normal conditions the "high-pressure" phase of symmetry Cmcm is obtained. This is in agreement with an earlier study of α-$FeSO_4$ by Frazer et al. [7] and by Samaras and Coing-Boyat (280 °C) [8]. Dehydration above 350 °C yielded increasing amounts of β-$FeSO_4$ and at 450 °C the pure β-phase was obtained. In all experiments an SO_2 atmosphere had to be used in the reaction vessel in order to avoid a decomposition of $FeSO_4$ into Fe_2O_3 and SO_2. These results give a mere reaction scheme according to

$$FeSO_4 \cdot 7\,H_2O \xrightarrow{T} \alpha\text{-}FeSO_4 \xrightarrow{T(350\,C)} \beta\text{-}FeSO_4\,.$$

It is not clear whether the α ↔ β transition is reversible at atmospheric pressure, although the following results obtained for the p–T diagram suggest that this is not the case.

3. X-Ray Diffraction Analysis

Powder X-ray diffraction measurements (radiation CuKα, $\lambda = 1.5418$ Å) on β-$FeSO_4$ (Table 1) lead uniquely to the space group Pbnm by the observed extinction conditions ($h0l$: $h + l = 2n$; $0hl$: $k = 2n$). Least-squares analysis of 25 peak positions gave

Table 1

X-ray powder diffraction pattern of β-$FeSO_4$ ($\lambda = 1.5418$ Å)

$h\ k\ l$	θ_{obs}	d_{obs}	d_{calc}	I_{obs}	I_{calc}
0 2 0	10.16	4.367	4.359	15.4	16.3
1 1 0	10.55	4.207	4.202	43.5	49
0 2 1	12.10	3.675	3.668	45.0	46.8
1 1 1	12.43	3.578	3.574	100.0	115
0 2 2	16.67	2.685	2.681	84.0	74
1 1 2	16.92	2.647	2.644	68.5	64.7
1 3 0	18.05	2.486	2.485	65.0	64
2 0 0	18.70	2.402	2.397	24.0	20.1
1 2 2	19.21	2.341	2.341	20.0	18.8
2 1 0	19.45	2.313	2.312	10.0	7.5
0 4 0	20.65	2.184	2.179	1.0	0.3
2 2 0	21.93	2.099	2.100	6.7	5.9
0 4 1	21.78	2.076	2.075	3.3	1.5
1 0 3	22.07	2.050	2.050	7.0	4.8
1 3 2	22.56	2.008	2.006	33.0	21.8
2 2 1			2.007		6.6
1 1 3	22.68	1.998	1.996	2.0	7.5
2 0 2	23.15	1.959	1.960	1.0	1.4
0 4 2	24.82	1.835	1.834	23.0	16.6
2 3 1	25.53	1.787	1.784	50.0	0.3
2 2 2			1.787		38.0
0 0 4	26.92	1.701	1.701	20.5	16.8
1 5 0	28.11	1.635	1.638	3.5	4.9
2 4 0	28.55	1.612	1.612	11.0	8.6
1 5 1	28.95	1.591	1.593	9.0	5.8
1 1 4	29.25	1.576	1.577	12.5	9.3
3 1 0	29.37	1.570	1.572	14.3	8.4
2 4 1			1.569		1.6
0 4 3			1.571		0.6

the lattice constants (the values for α-$FeSO_4$ are listed for comparison)

$$\beta\text{-FeSO}_4:\quad a = 4.795(2);\quad b = 8.715(5);\quad c = 6.804(4)\,,$$

$$\alpha\text{-FeSO}_4:\,[8]\; a = 5.252(5);\quad b = 7.978(8);\quad c = 6.590(10)\,.$$

This leads to $V = 284.3(2)$ Å^3, $V_{\mathrm{Mol}} = 42.81(2)$ cm^3/Mol and a calculated density of 3.55(3) g/cm^3 for β-$FeSO_4$ versus $V = 276.1$ Å^3 and $\varrho = 3.65$ g/cm^3 for α-$FeSO_4$. Hence there is a gain in volume by 3.0%, when going from the α- to the β-phase.

Table 2

The positional atomic parameters of β-$FeSO_4$

		X-ray results on 30 refl. $R = 6.0\%$			neutron diffraction results on 36 refl. $R = 4.8\%$		
Fe	4(a)	0.0	0.0	0.0	0.0	0.0	0.0
S	4(c)	0.481(8)	0.174(3)	0.25	0.512(19)	0.164(7)	0.25
01	4(c)	0.753(11)	0.121(7)	0.25	0.727(7)	0.115(4)	0.25
02	4(c)	0.463(17)	0.344(5)	0.25	0.450(9)	0.355(3)	0.25
03	8(d)	0.334(7)	0.126(4)	0.061(5)	0.313(5)	0.126(4)	0.071(3)

The positional parameters (Table 2) of the atoms were determined by least-squares calculations on the 25 observed intensities covering 30 reflections by the least-squares program POWLS [9]. The R-factor was 6%.

4. The p–T Phase Diagram of β-$FeSO_4$

First indications on polymorphism in $FeSO_4$ are reported by Hammel [10] and later by Pistorius in 1961 [11, 12], who observed a new quenchable phase of $FeSO_4$ at 5 kbar. Further experiments by Pistorius were hampered however by oxidation processes in the samples.

Our own experiments were carried out in a piston-cylinder-apparatus containing an internally heated solid medium pressure cell [3, 13, 14]. The experimental conditions were in the range up to 15 kbar and 800 °C. The holding times were between 2 and 48 h, starting materials were the α- and β-phases prepared by dehydration as described in Section 2. The samples were quenched to room temperature within about 10 s and then studied by X-ray diffraction. The results are summarized in Fig. 1. Within the studied p–T field the transformation

$$\beta\text{-FeSO}_4\ (\mathrm{Pbnm}) \overset{p}{\longleftrightarrow} \alpha\text{-FeSO}_4\ (\mathrm{Cmcm})$$

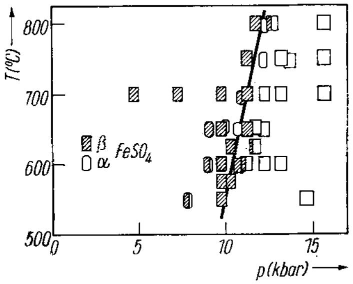

Fig. 1. The p–T phase diagram of $FeSO_4$. The starting phases (α, β-$FeSO_4$) are indicated

is reversible with an equilibrium phase boundary described by

$$T\ (^\circ\mathrm{C}) = 600 + 117.5\,[p\ (\mathrm{kb}) - 10.4]$$

and

$$\frac{\mathrm{d}p}{\mathrm{d}T} = 8.5\ (\mathrm{bar/deg})\,.$$

Below 550 °C the transition was found to be too sluggish to be followed. By extrapolation of the phase boundary one may conclude that β-$FeSO_4$ is the stable polymorph under normal conditions, while α-$FeSO_4$ is a metastable form when obtained by dehydration. The $\alpha \leftrightarrow \beta$ transition is connected with an increase of the molar volume $\Delta V = 1.23\ \mathrm{cm^3/Mol}$ comparing well with the corresponding $\Delta V = 1.14\ \mathrm{cm^3/Mol}$ in the homologue $MnSeO_4$ for example.

5. The Magnetic Structure of β-$FeSO_4$

The magnetic structure of the β-phase was determined by neutron diffraction at the DIDO research reactor in Jülich on a powdered sample prepared by dehydration at 700 °C. The sample size was 7 mm diameter and 30 mm height. The neutron wavelength used was 1.203 Å.

The room-temperature run yielded a well resolved diffraction pattern with 14 peaks comprising 36 reflections, which could be used for least-squares calculations with the program POWLS to calculate the structural atomic parameters. Refinement was carried to $R = 2.8\%$.

The results of the X-ray and neutron diffraction refinements are given in Table 2. Some differences in the positional parameters exceeding slightly the sum of the standard deviations may be understood from the roughly reciprocal relationship of the scattering factors of S and O for X-ray and neutron diffraction.

The diffraction diagram run at 4.2 K shows additional peaks arising from antiferromagnetic ordering of the Fe^{2+}-ions. All peaks of magnetic origin can be indexed on a unit cell doubled in a and b (Table 3)

Table 3

Comparison of observed and calculated magnetic neutron diffraction intensities at 4.2 K

h	k	l	I_{obs}	I_{calc}
$2a_0$	$2b_0$	c_0		
1	1	0	4950	4941
$\bar{1}$	3	0	1750	1745
1	5	0	700	612
1	1	2	2400	2328
$\bar{1}$	$\bar{1}$	$\bar{2}$		
$\bar{3}$	1	0		
$\bar{1}$	3	2	1700	1547
1	$\bar{3}$	2		
3	3	0		
$\bar{1}$	7	0	1350	1585
1	5	2		
$\bar{1}$	$\bar{5}$	2		
$\bar{3}$	5	0		
$\bar{3}$	1	2		
3	$\bar{1}$	2		

Fig. 2. The magnetic structure of β-FeSO$_4$ derived from neutron diffraction data

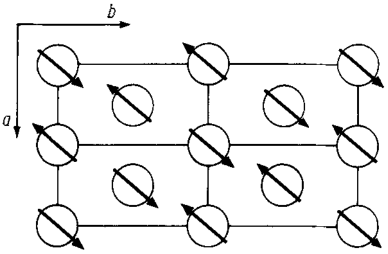

$$a_{\text{mag}} = 2a_{\text{chem}} ,$$
$$b_{\text{mag}} = 2b_{\text{chem}} ,$$
$$c_{\text{mag}} = c_{\text{chem}} .$$

Note, that in Table 3 the index l of all magnetic reflections is either zero or two. This means the Fe^{2+} sublattice could be described by $2a$, $2b$, $\frac{1}{2}c$.

The magnetic structure is shown in Fig. 2. We have ferromagnetic (110) planes with an antiferromagnetic propagation vector [110] in the ab-planes. The observed extinction rules allow components of the magnetic moments along the a- and the b-direction, however, zero components parallel to the c-axis. The result, derived from a least-squares fit of the measured magnetic intensities with the magnetic moment μ and the inclination angle α, is a collinear antiferromagnetic structure with the magnetic moments in the ab-plane inclined to the a-axis by $41 \pm 4°$.

The value of the magnetic moment is $5.44 \pm 0.27\mu_B$ at 4.2 K, compared to $\mu = 4.1\mu_B$ in α-FeSO$_4$. The intensities are listed in Table 3.

It is worth to emphasize, that the moments are inclined to the a-axis and the structure is yet collinear. This comes about, because the antiferromagnetic propagation vector is [110] (the moments are lying in (001) planes) and both components along the a- and b-axis change their signs simultaneously yielding a 180° rotation of the vector μ.

6. Magnetization Measurements

Results of the magnetization of β-FeSO$_4$ are shown in Fig. 3 for three different values of the magnetic field strength applied. It can be seen that in all cases the temperature dependence of the magnetization shows a cusp-like behaviour, indicative of a paramagnetic–antiferromagnetic transition near $T_N = 14$ K. In Fig. 4 we have plotted the temperature dependence of the reciprocal susceptibility (χ^{-1}). Curie-Weiss

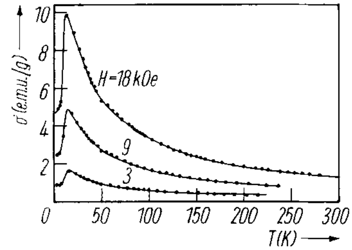

Fig. 3. Magnetization versus temperature of β-FeSO$_4$ in moderate magnetic fields

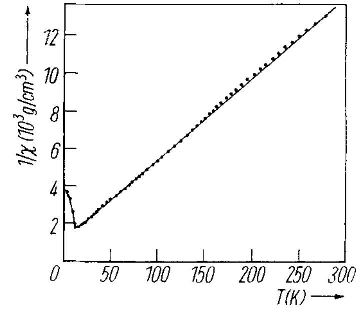

Fig. 4. Reciprocal susceptibility versus temperature for β-FeSO$_4$

behaviour is seen to be followed over almost the whole temperature region considered. From the slope of the χ^{-1} versus T curve an effective moment $\mu_{\text{eff}} = 5.32\mu_B/\text{Fe}$ is derived. The asymptotic Curie temperature is $\theta_p = -23$ K.

7. Discussion

The value $\mu_{\text{eff}} = 5.32\mu_B/\text{Fe}$ is significantly higher than the spin-only value ($4.90\mu_B/\text{Fe}$) expected for Fe^{2+}. It can be concluded therefore that the quenching of the orbital moment is incomplete in β-$FeSO_4$. Compared to the value of the effective moment derived for the paramagnetic state the value $\mu = 5.44\mu_B/\text{Fe}$ found in the magnetically ordered region appears rather high, since for $S = 2$ one expects $\mu/\mu_{\text{eff}} = S/\sqrt{S(S + 1)} \approx 0.82$. The origin of this discrepancy is not yet clear.

It was shown above that the magnetic structure of β-$FeSO_4$ is composed of ferromagnetic (110) planes with an antiferromagnetic propagation vector along [110]. The coupling of the Fe moments along the c-axis is ferromagnetic. A similar situation exists in $NiSO_4$ and in β-$FeSO_4$ where the magnetic moments are coupled ferromagnetically in the ac-plane and antiferromagnetically in the adjacent layers. In contrast to this are the results reported for α-$MnSO_4$ [6], α-$MnSeO_4$ [3], β-$MnSeO_4$ [5], β-$CuSO_4$ [15], and β-$CuSeO_4$ [16]. In α-$MnSO_4$ one has a cycloidal spiral arrangement, in all other compounds we observe a magnetic structure in which ferromagnetic (001) planes are coupled antiferromagnetically along [001] to the adjacent sheets. In all these compounds the nearest-neighbour distance between the 3d atoms is along the c-axis, and coupling can be understood by superexchange interaction via oxygen atoms [17]. The 3d atoms occupy positions in the center of a deformed octahedron of oxygen atoms. The octahedra belonging to adjacent 3d atoms have a common edge, so that chains of octahedra are formed in the c-direction. The (3d)-0-(3d) angle between two adjacent 3d atoms is 90° approximately, making superexchange between 3d atom neighbours in the same chain possible. For each two 3d atoms superexchange can take place via the O-atoms residing on the common octahedron edge. Apparently this superexchange leads to ferromagnetic coupling for Mn and Cu compounds. These findings are in keeping with the Goodenough-Kanamori rules [17]: In the series d^8, d^7, d^6, d^5 90°-superexchange is expected to be small and positive for the first members only. In case of d^5, however, levels of the type d_{xz} as well as d_{z^2} (or $d_{x^2-y^2}$) are magnetically occupied and can lead to a negative 90°-superexchange coupling. It is interesting to note that an analogous situation exists for the dichlorides of the 3d elements ($CdCl_2$ structure). Here chains of Cl-tetrahedra exist within the basal planes with two adjacent tetrahedra having a common edge. In these chains too superexchange is ferromagnetic for Ni and Fe but antiferromagnetic for Mn [18].

Acknowledgement

We acknowledge financial support by the Bundesministerium für Forschung und Technologie, 5300 Bonn, FRG, for the neutron diffraction experiments.

References

[1] H. Kamerlingh and A. Perrier, Commun. Kamerlingh Onnes Lab. Univ. Leiden **12**, 124a (1911).
H. Kamerlingh Onnes and E. Oosterhuis, Commnu. Kamerlingh Onnes Lab. Univ. Leiden **12**, 132c (1913).

[2] Magnetic Structure Data Sheets, issued by the Neutron Diffraction Commission of the International Union of Crystallography, Ed. D. Cox, BNL, Upton N.Y., USA (1974).

[3] A. Kirfel and G. Will, Internat. J. Magnetism **5**, 197 (1973).

[4] A. Kirfel and G. Will, High Temp.-High Pressures **6**, 525 (1974).
[5] H. Fuess and G. Will, J. appl. Phys. **39**, 628 (1968).
[6] G. Will, B. C. Fracer, G. Shirane, D. E. Cox, and P. J. Brown, Phys. Rev. **140**, A2139 (1965).
[7] B. C. Frazer and P. J. Brown, Phys. Rev. **125**, 1283 (1962).
[8] D. Samaras and J. Coing-Boyat, Bull. Soc. Franç. Minér. Crist. **93**, 190 (1970).
J. Coing-Boyat, Acta cryst. **12**, 939 (1959).
[9] W. Schäfer and G. Will, Z. Krist., in the press.
[10] F. Hammel, C. R. Acad. Sci. (France) **202**, 57 (1936).
[11] C. W. Pistorius, Naturwissenschaften **48**, 129 (1961).
[12] C. W. Pistorius, Z. Krist. **116**, 220 (1961).
[13] A. Neuhaus and R. Steffen, Z. phys. Chem. **73**, 128 (1970).
[14] A. Kirfel and A. Neuhaus, Z. phys. Chem. **91**, 121 (1974).
[15] I. Almdovar, B. C. Frazer, J. J. Hurst, D. C. Cox, and P. J. Brown, Phys. Rev. **138**, A153 (1965).
[16] W. Scharenberg and G. Will, J. Physique C1 **32**, 855 (1971).
[17] P. W. Anderson, in: Magnetism I, Ed. T. Rado and H. Suhl, Academic Press, New York 1963.
[18] M. M. Schieber, Experimental Magnetochemistry, Ed. E. P. Wohlfarth, North-Holland Publ. Co., Amsterdam 1967, Chapt. 7 and authors cited therein.

(Received November 23, 1976)